

Non-Val30Met mutation, septal hypertrophy, and cardiac denervation in patients with mutant transthyretin amyloidosis

Kyoko Hirakawa¹, Seiji Takashio^{1*}, Kyohei Marume¹, Masahiro Yamamoto¹, Shinsuke Hanatani¹, Eiichiro Yamamoto¹, Kenji Sakamoto¹, Yasuhiro Izumiya¹, Koichi Kaikita¹, Seitaro Oda², Daisuke Utsunomiya², Shinya Shiraishi², Mitsuharu Ueda³, Taro Yamashita³, Yasuyuki Yamashita², Yukio Ando³ and Kenichi Tsujita¹

¹Department of Cardiovascular Medicine, Graduate School of Medical Sciences, Kumamoto University, Kumamoto, Japan; ²Department of Diagnostic Radiology, Graduate School of Medical Sciences, Kumamoto University, Kumamoto, Japan; ³Department of Neurology, Graduate School of Medical Sciences, Kumamoto University, Kumamoto, Japan

Abstract

Aims Mutant transthyretin (ATTRm) amyloidosis is a systemic disease caused by the deposition of amyloid fibrils derived from mutated transthyretin. Although cardiac involvement impacts the prognosis of patients with ATTRm amyloidosis, the incidence of cardiac events, such as bradyarrhythmia, ventricular tachycardia, and heart failure, has not been fully elucidated. The aim of this study was to evaluate the prognosis and predictors of clinical outcomes, including cardiac events, in patients with ATTRm amyloidosis in Japan.

Methods and results We evaluated 90 consecutive patients with ATTRm amyloidosis at Kumamoto University. ATTRm amyloidosis was diagnosed by the observation of both amyloid fibril deposition on tissue biopsy and a transthyretin mutation on sequential analysis. Sympathetic nerve activity was evaluated in 59 patients using ¹²³I-iodine metaiodobenzylguanidine (¹²³I-MIBG) imaging. The endpoint was a composite of all-cause death, hospitalization for heart failure, and implantation of a pacemaker, implantable cardioverter defibrillator, or cardiac resynchronization therapy defibrillator. Sixty-seven patients had the Val30Met mutation (74%). The composite endpoint occurred in 23 patients (26%): all-cause death ($n = 6$), hospitalization for worsening heart failure ($n = 1$), and implantation of an implantable cardioverter defibrillator ($n = 6$), cardiac resynchronization therapy defibrillator ($n = 3$), or pacemaker ($n = 7$). The 5-year incident rate for clinical outcomes was 19%. In a multivariate Cox hazard analysis, age [hazard ratio (HR): 1.07, 95% confidence interval (95% CI): 1.01–1.12, $P = 0.015$], PQ interval (HR: 1.01, 95% CI: 1.00–1.02, $P = 0.042$), interventricular septum thickness in diastole (HR: 1.25, 95% CI: 1.09–1.42, $P = 0.001$), and non-Val30Met mutation (HR: 4.31, 95% CI: 1.53–12.16, $P = 0.006$) were independent predictive factors of clinical outcomes. Kaplan–Meier analysis demonstrated a significantly higher probability of the composite endpoint in the non-Val30Met group than in the Val30Met group (log-rank test: $P = 0.002$) and in patients with left ventricular hypertrophy than in patients without left ventricular hypertrophy (log-rank test: $P < 0.001$). In patients who underwent ¹²³I-MIBG imaging, a delayed heart-to-mediastinum (HM) ratio < 1.6 was a significant predictive factor of the composite endpoint (HR: 4.98, 95% CI: 1.73–14.37, $P = 0.003$) in the univariate Cox hazard analyses. Kaplan–Meier curve analysis showed that a delayed HM ratio < 1.6 was associated with a poor prognosis (log-rank test: $P = 0.001$).

Conclusions Non-Val30Met mutation, septal hypertrophy, and a delayed HM ratio are useful predictors of clinical outcomes in patients with ATTRm amyloidosis in Japan. These results suggest that it is important to evaluate cardiac involvement in terms of morphological (left ventricular hypertrophy) and functional (cardiac denervation) perspectives using echocardiography and ¹²³I-MIBG imaging, respectively.

Keywords Mutant transthyretin amyloidosis; Clinical outcome; Cardiac prognosis; ¹²³I-MIBG imaging; Val30Met mutation

Received: 3 April 2018; Revised: 30 August 2018; Accepted: 2 September 2018

*Correspondence to: Seiji Takashio, Department of Cardiovascular Medicine, Graduate School of Medical Sciences, Kumamoto University, Honjo, Kumamoto 860-8556, Japan. Tel: +81 96 373 5175; Fax: +81 96 362 3256. Email: s-takash@kumamoto-u.ac.jp

Introduction

Amyloidosis is a systemic disease caused by the extracellular deposition of misfolded protein fibrils, leading to progressive organ dysfunction.¹ Transthyretin (TTR) is a major amyloidogenic protein that forms a homotetramer and acts as a plasma transport protein for thyroid hormones and retinol-binding protein with vitamin A. In patients with transthyretin amyloidosis (ATTR), amyloid fibrils, consisting of TTR monomers, dissociate from destabilized TTR tetramers. Depending on the presence or absence of a genetic mutation, ATTR is classified into two types: mutant ATTR (ATTRm) amyloidosis and wild-type ATTR.^{2,3}

Mutant ATTR was once believed to be a rare autosomal dominant disease, restricted to an endemic presence in specific areas; however, with the progression of molecular and biochemical analyses, it has become clear that this disease occurs worldwide. Although the Val30Met mutation is most prevalent type of mutation in ATTRm amyloidosis in Japan, many other TTR mutations exist.⁴ To date, over 140 TTR mutations have been identified,⁵ with ATTRm amyloidosis symptoms varying according to the TTR mutation.⁶ ATTR symptoms are linked to the deposition of amyloid fibrils in several organs, for example, sensorimotor polyneuropathy, gastrointestinal tract disorders, and heart and kidney failure.^{7–10} In particular, cardiac involvement causes heart failure and cardiac arrhythmias due to infiltrative and restrictive cardiomyopathy and impacts the prognosis of patients with ATTR.^{8–11}

Because TTR-derived amyloid fibril deposition causes peripheral and autonomic polyneuropathy, it is reasonable to speculate that the cardiac neuronal homeostasis is altered in patients with ATTRm amyloidosis. A reduced heart-to-mediastinum uptake (HM) ratio on 123-iodine metaiodobenzylguanidine (¹²³I-MIBG) imaging, which is a noninvasive tool for assessing cardiac sympathetic nerve activity, has been reported to predict a poor prognosis in patients with ATTRm amyloidosis.¹² However, these previous reports did not evaluate cardiac events, such as worsening heart failure and/or the implantation of cardiac devices. In addition, these previous studies were conducted in western countries, and racial differences in cardiac phenotypes were not evaluated. Therefore, in the present study, we investigated the prognosis and predictors of clinical outcomes in patients with ATTRm amyloidosis in Japan.

Methods

Study population

We retrospectively reviewed 95 consecutive patients with ATTRm amyloidosis who visited the Department of Neurology at Kumamoto University Hospital between July 1994 and

April 2017. ATTRm amyloidosis was diagnosed by the observation of both amyloid fibril deposition on tissue biopsy (abdominal subcutaneous adipose tissue, skin, or gastrointestinal tract) and a TTR mutation on sequential analysis.¹³ Patient characteristics, clinical evaluations, and clinical outcomes were analysed. Three patients were excluded because a pacemaker had already been implanted at the time of the diagnosis of ATTRm amyloidosis, and two patients were lost to follow-up. Finally, we evaluated 90 patients with ATTRm amyloidosis. The study was conducted in accordance with the principles outlined in the Declaration of Helsinki, and the study protocol was approved by the Human Ethics Review Committee of Kumamoto University (no. 1324).

Cardiovascular evaluations

Electrocardiography (ECG), echocardiography, and laboratory data at the time of the diagnosis were collected. Echocardiography was performed using commercially available ultrasound equipment. Cardiac involvement was defined by increased wall thickness [interventricular septum thickness in diastole (IVSTd) ≥ 12 mm] on echocardiography in the absence of any other cause of ventricular hypertrophy.^{7,14} The left ventricular ejection fraction (LVEF) was calculated using the modified Simpson's method. Early (E) and late atrial (A) transmitral peak flow velocities were measured from the mitral inflow velocities. The peak early diastolic velocity on the septal corner of the mitral annulus (e') was determined by pulsed-wave tissue Doppler imaging, and the E/e' was calculated. Among the included patients, B-type natriuretic peptide (BNP) was measured in 69 patients.

A total of 61 patients underwent ¹²³I-MIBG imaging at diagnosis, starting in 2009. We excluded two patients because of lost to follow-up. Finally, we evaluated 59 patients. Anterior planar images were obtained at 15 min (early images) and 3 h (delayed images) after the intravenous injection of 111 MBq (3 mCi) of ¹²³I-MIBG (FUJIFILM RI Pharma Co., Ltd., Tokyo, Japan). The images were acquired with a dual-headed gamma camera equipped with a low-medium energy general purpose collimator (Symbia T16, Siemens, CO., Ltd., Berlin, Germany). The image acquisition time was 5 min, matrix size was 256 \times 256, zoom was 1.23, and the energy window was set at 159 keV ($\pm 7.5\%$). The pixel size was 1.95 mm. Using the region of interest (ROI) method, we calculated the early and delayed HM ratios on anterior views of the planar images. An irregular circular ROI was manually drawn on the left ventricle, and a square ROI was placed in the upper mediastinum area. The standardization of the HM ratio reported by Nakajima *et al.*^{15,16} was used, and early and delayed HM ratios, and the washout rate, were calculated. The HM ratio was considered to be reduced if it was below 1.60 based on previous studies.¹²

Clinical follow-up

We evaluated the incidence of a composite endpoint, defined as all-cause death; hospitalization due to worsening heart failure; and implantation of a cardiac resynchronization therapy defibrillator (CRT-D), implantable cardioverter defibrillator (ICD), or pacemaker due to a second-degree or third-degree atrioventricular block and sick sinus syndrome with symptoms. An ICD was implanted for primary prevention after a multidisciplinary team assessed the fatal ventricular arrhythmia risk if the patient had non-sustained ventricular tachycardia. A CRT-D was implanted based on the current European Society of Cardiology guidelines.^{17,18} Mortality and cardiovascular events were identified by a search of the medical records, and were confirmed by a questionnaire and direct contact via a telephone interview of the patient or a family member, if deceased.

Statistical analysis

Normally distributed data are presented as means \pm standard deviation or medians (interquartile range), and group differences were evaluated using the Student's *t*-test or Mann–Whitney *U*-test. Categorical values are presented as numbers (percentage), and group differences were evaluated using the χ^2 or Fisher's exact test, as appropriate. Variables with a skewed distribution were first logarithmically transformed prior to univariate linear regression analyses. Univariate Cox hazard analyses were performed to identify parameters significantly related to the composite endpoint. A multivariate Cox hazard analysis was performed using a forward stepwise model ($P < 0.10$ for entry and $P < 0.05$ to remain). Because the BNP level and delayed HM ratio had some missing values, we did not enter these factors into the multivariate model. Kaplan–Meier curves for the composite endpoint were constructed, and group differences were evaluated using the log-rank test. A two-tailed *P* value of 0.05 was considered statistically significant. All statistical analyses were performed using SPSS version 23 software (IBM Corp., Armonk, NY).

Results

Patient characteristics and clinical outcomes

Table 1 shows the patient characteristics for the total study population. During a median follow-up period of 6.0 ± 6.3 years, the composite endpoint occurred in 23 patients (25.6%; event group). Details of the composite endpoint are as follows: all-cause death ($n = 6$), hospitalization for worsening heart failure ($n = 1$), and implantation of an

ICD ($n = 6$), CRT-D ($n = 3$), or pacemaker ($n = 7$). All of the patients who had symptomatic bradyarrhythmia had pacemaker implantation. The 5-year incident rate of clinical outcomes was 19%. An LVEF $< 50\%$ was observed in only nine patients (10%). An IVSTd > 12 mm was observed in 44 patients (49%). The median BNP level was 99.6 pg/mL, and a BNP level > 100 pg/mL was observed in 15 patients (17%). In addition, the proportions of the observed ATTR gene mutations are shown in Figure 1. A total of 67 patients (74.4%) had the Val30Met mutation, and many other known ATTR mutations in Japan were observed. Among the patients with the Val30Met mutation, 35 patients were classified as early onset (defined as a disease onset at or before 50 years of age). A total of 42 patients (47%) underwent ^{99m}Tc-labelled pyrophosphate scintigraphy. Among these, 21 patients had a left ventricular (LV) wall thickness > 12 mm, approximately 90% of whom ($n = 19$) were positive for ^{99m}Tc-pyrophosphate scintigraphy.

Age and the age at onset were significantly older in the event group compared with those in the event-free group (age: $P < 0.001$; age at onset: $P < 0.001$). On ECG, the event group had a longer PQ interval and QRS duration compared with those in the event-free group (PQ interval: $P = 0.020$; QRS duration: $P = 0.032$). On echocardiography, the event group had significantly increased LV wall thickening and E/e', and significantly worse LVEF, compared with those in the event-free group (IVSTd: $P < 0.001$; E/e': $P < 0.001$; LVEF: $P < 0.001$). In addition, BNP levels were higher in the event group compared with those in the event-free group ($P < 0.001$). Almost all patients ($n = 87$) were treated by anti-amyloid therapy; 49 patients were treated by tafamidis, five patients were treated by other anti-amyloid drugs (diflunisal), and 33 patients underwent liver transplantation. The patients treated by tafamidis had the highest clinical event rate [tafamidis, $n = 17$ (34.7%); liver transplantation, $n = 41$ (12.1%)], as the patients who were treated by tafamidis were unable to undergo liver transplantation because of advanced age (tafamidis vs. liver transplantation: 60.6 ± 14.2 vs. 48.2 ± 9.6 years old, $P < 0.01$) or organ failure, including heart failure.

Prognostic factors in mutant transthyretin amyloidosis

Table 2 shows the results of the univariate and multivariate Cox hazard analyses for the composite endpoint. In the multivariate analysis, age [hazard ratio (HR): 1.07, 95% confidence interval (CI): 1.01–1.12, $P = 0.015$], non-Val30Met mutation (HR: 4.31, 95% CI: 1.53–12.16, $P = 0.006$), PQ interval (HR: 1.01, 95% CI: 1.00–1.02, $P = 0.042$), and IVSTd (HR: 1.25, 95% CI: 1.09–1.42, $P = 0.001$) were independently associated with the composite endpoint. Figure 2 shows the Kaplan–Meier curve for the probability of the composite endpoint among all study participants. In addition, the participants were

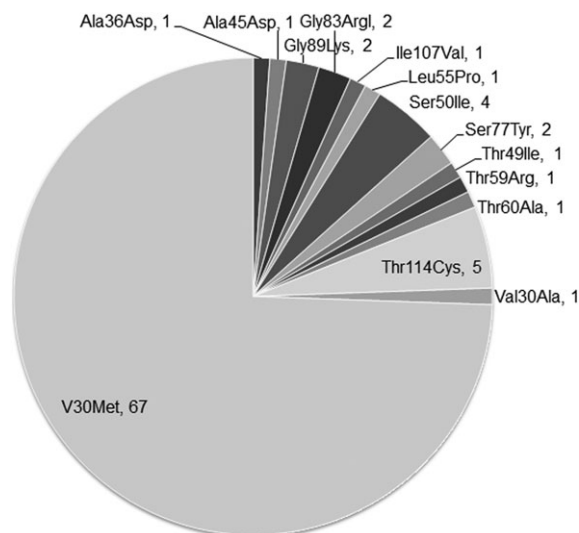
Table 1 Patient characteristics in the total study population according to the clinical outcome

	All patients, <i>n</i> = 90	Event (–), <i>n</i> = 67	Event (+), <i>n</i> = 23	<i>P</i> value
Age (year)	56.7 ± 14.1	53.1 ± 14.0	67.3 ± 7.9	<0.001
Male (yes, %)	50 (55.6)	34 (50.7)	16 (69.6)	0.117
Val30Met (yes, %)	67 (74.4)	53 (79.1)	14 (60.9)	0.084
Age of onset (year)	49.3 ± 15.9	45.2 ± 15.7	60.9 ± 9.3	<0.001
PQ interval (ms)	184.9 ± 44.6	177.5 ± 46.2	205.4 ± 32.6	0.020
QRS duration (ms)	104.7 ± 23.8	99.5 ± 19.0	118.8 ± 30.0	0.032
LVDd (mm)	41.4 ± 4.9	41.5 ± 4.6	40.9 ± 5.7	0.222
LVDs (mm)	26.4 ± 4.9	25.8 ± 5.0	28.1 ± 4.4	0.056
IVSTd (mm)	12.6 ± 3.9	11.4 ± 3.5	16.0 ± 3.1	<0.001
PWTd (mm)	12.2 ± 3.6	10.8 ± 2.8	15.8 ± 2.9	<0.001
LVEF (%)	61.6 ± 8.1	62.8 ± 8.1	58.1 ± 7.5	<0.001
E/A	1.3 ± 0.8	1.4 ± 0.8	1.2 ± 0.8	0.071
E/e'	13.9 ± 7.0	12.4 ± 6.3	18.2 ± 6.8	<0.001
Albumin (mg/dL)	4.0 ± 0.5	4.0 ± 0.5	3.9 ± 0.4	0.462
Creatinine (mg/dL)	0.7 ± 0.2	0.7 ± 0.2	0.8 ± 0.2	0.032
eGFR (mL/min/1.73 m ²)	87.8 ± 26.3	92.7 ± 27.2	75.0 ± 18.7	0.007
Haemoglobin (g/dL)	12.9 ± 1.16	13.0 ± 1.2	12.9 ± 1.1	0.667
BNP (pg/mL) (<i>n</i> = 69)	99.2 (55.4–93.4)	79.1 (38.8–75.8)	142.0 (71.5–157.0)	<0.001
hs-cTnT (ng/mL) (<i>n</i> = 52)	0.028 (0.022–0.038)	0.030 (0.028–0.043)	0.020 (0.017–0.025)	0.171

¹²³ I-MIBG imaging	All patients, <i>n</i> = 59	Event (–) <i>n</i> = 41	Event (+) <i>n</i> = 18	<i>P</i> value
Age (years)	59.0 ± 15.1	54.9 ± 16.0	68.3 ± 6.5	0.003
Male (<i>n</i> , %)	38 (64.4)	24 (58.5)	14 (77.8)	0.155
Val30Met (<i>n</i> , %)	44 (74.6)	34 (82.9)	10 (55.6)	0.026
Age of onset (years)	53.3 ± 15.7	48.9 ± 16.6	63.3 ± 6.0	0.004
PQ interval (ms)	190.8 ± 38.0	181.1 ± 37.1	211.8 ± 31.4	0.003
QRS duration (ms)	105.5 ± 22.8	98.7 ± 15.7	120.6 ± 28.7	0.014
IVSTd (mm)	12.9 ± 3.8	11.4 ± 3.1	16.2 ± 3.2	<0.001
LVEF (%)	61.0 ± 8.0	62.7 ± 7.8	57.2 ± 7.3	0.004
E/e'	13.5 ± 6.5	11.5 ± 5.3	18.2 ± 6.6	<0.001
BNP (pg/mL)	54.6 (35.4–78.3)	39.0 (18.9–73.6)	66.1 (56.7–116.5)	0.030
Early HM ratio	2.3 ± 0.6	2.4 ± 0.6	2.1 ± 0.7	0.052
Delayed HM ratio	2.1 ± 0.8	2.2 ± 0.8	1.7 ± 0.8	0.022
Washout ratio	49.7 ± 33.1	44.6 ± 14.2	61.4 ± 55.3	0.270

BNP, B-type natriuretic peptide; eGFR, estimated glomerular filtration rate; hs-cTnT, high-sensitivity cardiac troponin T; HM, ¹²³I-MIBG heart-to-mediastinum uptake; IVSTd, intraventricular septal thickness in diastole; LVDd, left ventricular diastolic dimension; LVDs, left ventricular systolic dimension; LVEF, left ventricular ejection fraction; PWTd, posterior wall thickness in diastole; ¹²³I-MIBG, ¹²³iodine metaiodobenzylguanidine.

Data are presented as mean ± standard deviation, *n* (%), or median (interquartile range).

Figure 1 TTR mutations observed in the present study.

divided into groups according to TTR mutation (Val30Met vs. non-Val30Met) and IVSTd (≤ 12 vs. > 12 mm). The Kaplan–Meier analysis demonstrated a significantly higher probability of the composite endpoint in the non-Val30Met group compared with that in the Val30Met group (log-rank test: $P = 0.002$) and in patients with LV hypertrophy, defined as an IVSTd ≥ 12 mm, compared with that in patients without LV hypertrophy (log-rank test: $P < 0.001$) (Figure 3A and B).

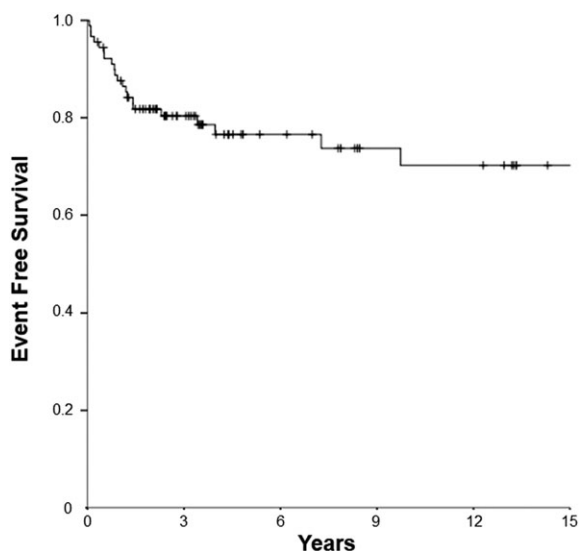
Among the 67 patients with the Val30Met mutation, the composite endpoint occurred in 14 patients (21%). Univariate Cox hazard analyses of the composite endpoint among patients with Val30Met mutation revealed the same tendencies as those in the analysis of all study participants; age, QRS duration, IVSTd, E/e', and circulation levels of creatinine were significant predictors of the composite endpoint among Val30Met patients (data not shown).

Furthermore, we performed additional analyses on a limited endpoint that excluded device implantation (all-cause death and hospitalization for worsening heart failure). This

Table 2 Results of univariate and multivariate Cox hazard analyses of clinical outcome predictors in the total study population

Variables	Univariate			Multivariate		
	HR	95% CI	P value	HR	95% CI	P value
Age (years)	1.08	1.14–1.12	<0.01	1.07	1.01–1.12	0.015
Male (yes)	2.16	0.88–5.28	0.093	Not selected		
Non-Val30Met mutation (yes)	3.23	1.38–8.02	0.012	4.31	1.53–12.16	0.006
PQ interval (ms)	1.01	1.00–1.02	<0.01	1.01	1.00–1.02	0.042
QRS duration (ms)	1.03	1.01–1.04	<0.01	Not selected		
IVSTd (mm)	1.32	1.19–1.47	<0.01	1.25	1.09–1.42	0.001
LVEF (%)	0.94	0.90–0.98	<0.01	Not selected		
E/e'	1.07	1.02–1.13	0.004	Not selected		
Creatinine (mg/dL)	8.96	1.42–56.79	0.020	Not selected		
Ln BNP (<i>n</i> = 69)	2.62	1.14–6.00	0.023	Not selected		
Ln hs-cTnT (<i>n</i> = 52)	5.42	0.99–29.7	0.052			
Delayed HM ratio <1.6	4.98	1.73–14.37	0.003			

CI, confidence interval; HR, hazard ratio; hs-cTnT, high-sensitivity cardiac troponin T; IVSTd, intraventricular septal thickness in diastole; Ln, log-transformed; LVEF, left ventricular ejection fraction.

Figure 2 Kaplan–Meier curve depicting the probability of clinical outcomes in all patients with mutant transthyretin amyloidosis.

endpoint occurred in 12 patients (13%) (all-cause death, *n* = 8; hospitalization for worsening heart failure, *n* = 4). The 5-year event-free rate was 86.9%. Univariate cox hazard analyses revealed the following predictors of this limited endpoint as follows: age, male sex, non-Val30Met mutation, IVSTd, LVEF, E/e', and the levels of creatinine, estimated glomerular filtration rate, and high-sensitivity cardiac troponin T. We could not perform a multivariate analysis because of the low incidence of this limited endpoint (data not shown).

Prognostic utility of ¹²³I-MIBG scintigraphy

The characteristics of the 59 patients who underwent ¹²³I-MIBG scintigraphy are shown in *Table 1*. As in the analysis of the total study population, age and age at onset were

significantly older in the event group compared with that in the event-free group (age: *P* = 0.003; age at onset: *P* = 0.004). Non-Val30Met mutation was more frequently observed in the event group than in the event-free group (*P* = 0.026). On ECG, the event group had a longer PQ interval and QRS duration compared with those in the event-free group (PQ interval: *P* = 0.003; QRS duration: *P* = 0.014). On echocardiography, the event group had significantly increased LV wall thickening and E/e', and significantly worse LVEF, compared with those in the event-free group (IVSTd: *P* < 0.001; E/e': *P* < 0.001; LVEF: *P* = 0.004). BNP levels were higher in the event group compared with that in the event-free group (*P* = 0.030). The average delayed HM ratio was 2.1 ± 0.8 across all patients with ¹²³I-MIBG scintigraphy data and was significantly lower in the event group compared with that in the event-free group (1.7 ± 0.8 vs. 2.2 ± 0.8 , *P* = 0.022).

The delayed HM ratio was significantly correlated with the LVEF and was significantly inversely correlated with age, IVSTd, E/e', and the circulating BNP level in the univariate linear regression analyses (*Table 3*; Supporting Information, *Figure S1*). In the univariate Cox hazard analyses, a delayed HM ratio < 1.6 was a significant predictive factor of the composite endpoint (HR: 4.98, 95% CI: 1.73–14.37, *P* = 0.003; Supporting Information, *Table S1*). Kaplan–Meier curve analysis showed that a delayed HM ratio < 1.6 is associated with a poor prognosis (log-rank test: *P* = 0.001; *Figure 3C*).

Discussion

The major findings of the present study are as follows: (i) the 5-year incident rate of clinical outcomes was 19% in patients with ATTRm amyloidosis in Japan; (ii) non-Val30Met mutation and LV hypertrophy (IVSTd > 12 mm) were significant predictive factors of clinical outcomes; and (iii) the delayed HM ratio was significantly correlated with LV wall thickness, and a low delayed HM ratio (>1.6) was an independent

Figure 3 Kaplan–Meier curves depicting the probability of clinical outcomes in subgroups based on (A) *TTR* mutation, (B) left ventricular hypertrophy, and (C) delayed heart-to-mediastinum (HM) ratio. IVSTd, intraventricular septal thickness in diastole.

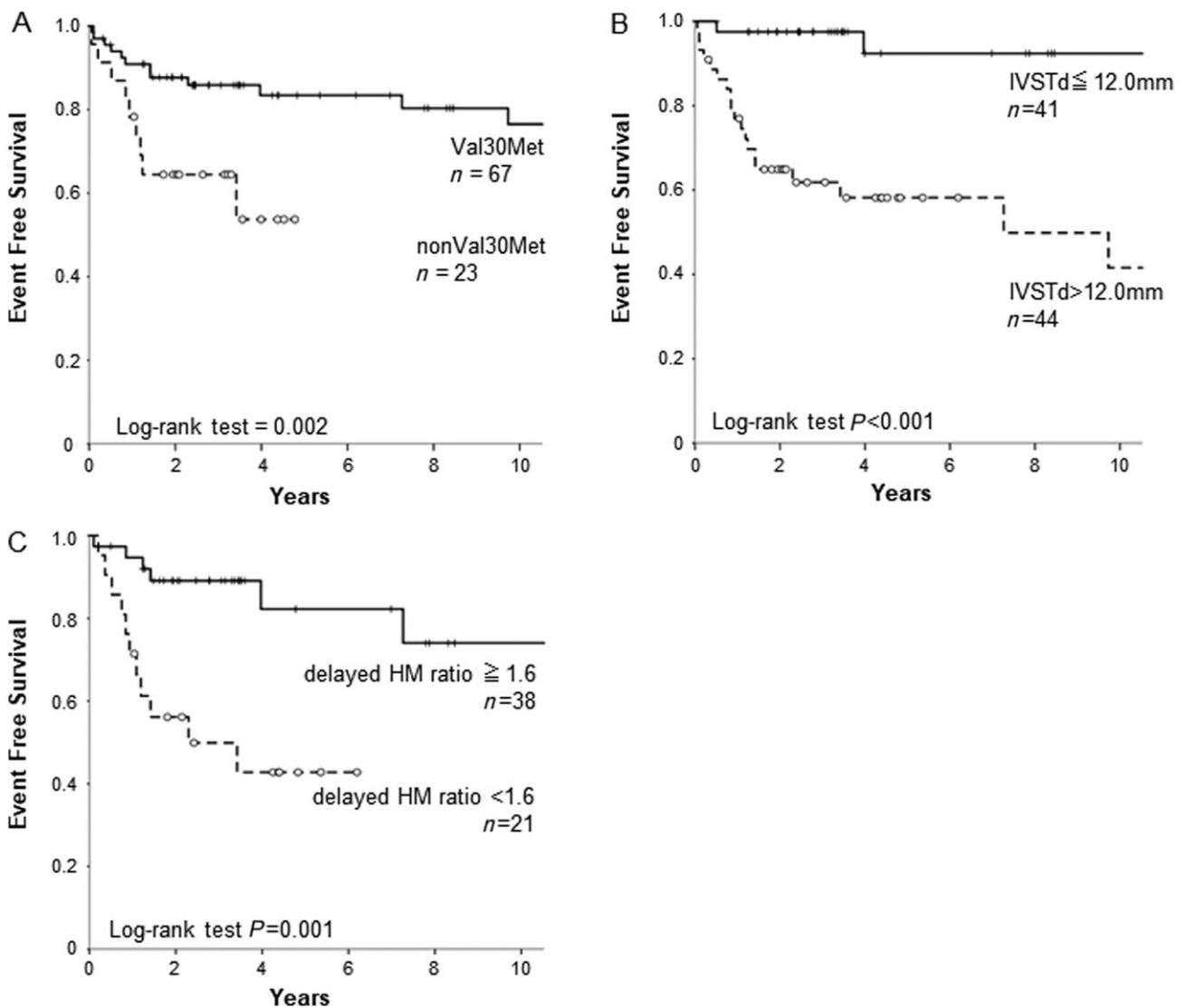


Table 3 Result of the univariate linear regression analysis for the delayed HM ratio

Factors	<i>r</i>	<i>P</i> value
Age (years)	−0.357	0.005
PQ interval (ms)	−0.191	0.155
QRS duration (ms)	−0.014	0.920
LVEF (%)	0.336	0.009
IVSTd (mm)	−0.562	<0.001
E/A	0.217	0.116
E/e′	−0.426	0.001
Creatinine (mg/dL)	−0.072	0.589
Haemoglobin (g/dL)	0.139	0.297
Ln BNP	−0.511	<0.001

IVSTd, intraventricular septal thickness in diastole; Ln, log-transformed; LVEF, left ventricular ejection fraction.

predictor of poor clinical outcomes. Together, these results indicate that the type of genetic mutation, presence of LV hypertrophy, and delayed HM ratio are useful predictors of clinical outcomes in Japanese patients with ATTRm amyloidosis. To our knowledge, the present study is the first to demonstrate the incidence of cardiac events and prognostic factors, with a long follow-up duration (median follow-up period, 6.0 years), in patients with ATTRm amyloidosis in Japan.

Previous studies have shown that ¹²³I-MIBG imaging is useful in predicting a poor prognosis in patients with ATTRm amyloidosis. Although the endpoint of these previous studies was all-cause death, the main cause of death was cachexia or surgical death. Other studies have analysed the prognostic

utility of ^{123}I -MIBG imaging among patients with only Val30Met ATTRm amyloidosis.¹² Furthermore, Ruberg *et al.*¹⁹ previously demonstrated that ATTRm amyloidosis with Val122Ile mutation is associated with worse morbidity and mortality, and a higher cardiovascular hospitalization rate, compared with those in wild-type ATTR. However, this previous study had a very small sample size and was limited to the Val122Ile mutation. Furthermore, many studies of ATTRm amyloidosis have been conducted in Europe¹¹ or the USA,²⁰ which have different TTR mutation and phenotype patterns from those in Japan. Thus, there are no previous reports on the clinical outcomes (including cardiac events) and their predictors in a large number of Japanese patients with various TTR mutations in ATTRm amyloidosis. The present study is first to report on the prognosis of patients with ATTRm amyloidosis in Japan. We believe that this study provides useful clinical information and can improve cardiac management, not only in Japanese patients with ATTRm amyloidosis but also in patients worldwide.

In the present study, 74% of patients had the Val30Met mutation. This mutation is found worldwide and is the most common TTR mutation in the world. Val30Met mutation, particularly in patients with early-onset Val30Met ATTRm amyloidosis, is characterized by a predominant loss of superficial sensation. However, a previous study revealed that cardiomyopathy is observed in 43% of patients with Val30Met amyloidosis.⁷ Consistent with this, cardiomyopathy, defined as an IVSTd > 12 mm, was observed in 27 patients (40.3%) in the present study. Because cardiac amyloidosis is not rare in patients with the Val30Met mutation and LV hypertrophy is significantly correlated with cardiac events, it is important to evaluate the progression of cardiomyopathy via consecutive echocardiographic monitoring.

Left ventricular hypertrophy indicates the deposition of amyloid fibrils in the heart, based on a morphological evaluation of cardiac amyloidosis. We additionally evaluated cardiac denervation using ^{123}I -MIBG imaging. In the present study, the delayed HM ratio was inversely correlated with the IVSTd, and a low delayed HM ratio was associated with a high clinical event rate. In a pioneering study on patients with Val30Met amyloidosis using ^{123}I -MIBG imaging, Tanaka *et al.*²¹ demonstrated that cardiac denervation might occur before LV wall thickening or clinically apparent heart disease. In addition, several studies have demonstrated that the delayed HM ratio correlates negatively with the severity of polyneuropathy.^{22,23} This observation suggests that cardiac denervation is present prior to cardiac hypertrophy. Thus, ^{123}I -MIBG imaging should be considered if advanced polyneuropathy manifests, even if LV hypertrophy is not observed, to evaluate the cardiac involvement.

Recently, new drugs for ATTRm amyloidosis therapy have been developed, such as those for TTR stabilization (diflunisal²⁴ and tafamidis²⁵) and the suppression of TTR production (siRNA²⁶), improving the neuropathic prognosis of patients with ATTRm amyloidosis. Although these therapies are expected to decrease cardiac events, a prior study

showed an absence of significant changes in biochemical and echocardiographic parameters with tafamidis therapy for ATTR-related cardiomyopathy.²⁷ As LV hypertrophy and cardiac denervation were revealed to be useful predictive factors of clinical outcomes in the present study, the evaluation of these parameters using reproducible methods, such as cardiac magnetic resonance imaging and ^{123}I -MIBG, may act as reliable surrogate makers for clinical outcomes in determining the efficacy of new TTR drugs. However, further evaluation is necessary to confirm this point.

The present study has several limitations to acknowledge. First, ATTRm amyloidosis is a rare disease, even in our endemic area; thus, the sample size was relatively small. Second, we defined the composite endpoint as all-cause mortality, hospitalization for heart failure, and device implantation, including an ICD for primary prevention. The indication of an ICD for primary prevention in patients with ATTRm amyloidosis is still controversial. As mentioned previously, a multidisciplinary team assessment of the risk of fatal ventricular arrhythmia was performed if the patient had non-sustained ventricular tachycardia. Unfortunately, we could not evaluate the incidence of appropriate ICD discharges because we did not follow-up all of the patients with an ICD/CRT-D at our institution. It is necessary to evaluate the risk stratification of future fatal ventricular tachycardia and the appropriate ICD implantation criteria in patients with ATTRm amyloidosis in further studies. Third, there are some biases inherent to observational studies. ^{123}I -MIBG scintigraphy scanning depended on the judgement of the physicians and was obtained in only 59 patients. Therefore, we could not include these parameters in the multivariate analysis of the cardiac prognostic factors in ATTRm amyloidosis. Finally, the study design was retrospective in nature. Further prospective studies of larger groups are needed to confirm the present results.

In conclusion, the present results indicate that non-Val30Met mutation, the presence of LV hypertrophy, and a low delayed HM ratio are useful predictive factors of clinical outcomes in patients with ATTRm amyloidosis in Japan. These results suggest that it is important to evaluate cardiac involvement in terms of morphological (LV hypertrophy) and functional (cardiac denervation) perspectives using echocardiography and ^{123}I -MIBG imaging, respectively.

Conflict of interest

None declared.

Funding

This work was supported by Grants-in-Aid for Young Scientists B from the Japan Society for the Promotion of Science (S.T.; 17K16015).

Supporting information

Additional supporting information may be found online in the Supporting Information section at the end of the article.

Figure S1. The scatterplots show the relationship between the delayed HM ratio in ¹²³I-MIBG scintigraphy and (A) age, (B) LVEF, (C) IVSTd, (D) E/e', and (E) Ln BNP, as assessed in linear regression analyses.

¹²³I-MIBG: 123-iodine metaiodobenzylguanidine, HM: ¹²³I-MIBG heart-to-mediastinum uptake, LVEF: left ventricular ejection fraction, IVSTd: intraventricular septal thickness in diastole, Ln BNP: log-transformed B-type natriuretic peptide.

Table S1. Results of the univariate Cox hazard analyses for clinical outcome predictors in patients who underwent ¹²³I-MIBG imaging (n=59).

References

- Falk HR, Comenzo LR, Skinner M. The systemic amyloidoses. *N Engl J Med* 1997; **337**: 898–909.
- Sperry BW, Vranian MN, Hachamovitch R, Joshi H, Ikram A, Phelan D, Hanna M. Subtype-specific interactions and prognosis in cardiac amyloidosis. *J Am Heart Assoc* 2016; **5**: e002877.
- Rapezzi C, Merlini G, Quarta CC, Riva L, Longhi S, Leone O, Salvi F, Ciliberti P, Pastorelli F, Biagini E, Coccolo F, Cooke RM, Bacchi-Reggiani L, Sangiorgi D, Ferlini A, Cavo M, Zamagni E, Fonte ML, Palladini G, Salinaro F, Musca F, Obici L, Branzi A, Perlini S. Systemic cardiac amyloidoses: disease profiles and clinical courses of the 3 main types. *Circulation* 2009; **120**: 1203–1212.
- Ueda M, Ando Y. Recent advances in transthyretin amyloidosis therapy. *Transl Neurodegener* 2014; **3**: 19.
- Yamashita T, Ueda M, Misumi Y, Masuda T, Nomura T, Tasaki M, Takamatsu K, Sasada K, Obayashi K, Matsui H, Ando Y. Genetic and clinical characteristics of hereditary transthyretin amyloidosis in endemic and non-endemic areas: experience from a single-referral center in Japan. *J Neurol* 2018; **265**: 134–140.
- Sekijima Y. Transthyretin (ATTR) amyloidosis: clinical spectrum, molecular pathogenesis and disease-modifying treatments. *J Neurol Neurosurg Psychiatry* 2015; **86**: 1036–1043.
- Gertz MA, Benson MD, Dyck PJ, Grogan M, Coelho T, Cruz M, Berk JL, Plante-Bordeneuve V, Schmidt HHJ, Merlini G. Diagnosis, prognosis, and therapy of transthyretin amyloidosis. *J Am Coll Cardiol* 2015; **66**: 2451–2466.
- Semigran MJ. Transthyretin amyloidosis. *J Am Coll Cardiol* 2016; **68**: 173–175.
- Kristen AV, Scherer K, Buss S, aus dem Siepen F, Haufe S, Bauer R, Hinderhofer K, Giannitsis E, Hardt S, Haberkorn U, Katus HA, Steen H. Non-invasive risk stratification of patients with transthyretin amyloidosis. *JACC Cardiovasc Imaging* 2014; **7**: 502–510.
- Izumiya Y, Takashio S, Oda S, Yamashita Y, Tsujita K. Recent advances in diagnosis and treatment of cardiac amyloidosis. *J Cardiol* 2018; **71**: 135–143.
- Klaassen SHC, Klaassen B, Tromp J, Nienhuis HLA, van der Meer P, van der Berg MP, Blokzijl H, van Veldhuisen DJ, Hazenberg BPC. Frequency of and prognostic significance of cardiac involvement at presentation in hereditary transthyretin-derived amyloidosis and the value of N-terminal pro-B-type natriuretic peptide. *Am J Cardiol* 2018; **121**: 107–112.
- Coutinho MC, Cortez-Dias N, Cantinho G, Conceicao I, Oliveira A, Bordalo e Sa A, Goncalves S, Almeida AG, de Carvalho M, Diogo AN. Reduced myocardial 123-iodine metaiodobenzylguanidine uptake: a prognostic marker in familial amyloid polyneuropathy. *Circ Cardiovasc Imaging* 2013; **6**: 627–636.
- Ando Y, Ohlsson P-I, Suhr O, Nyhlin N, Yamashita T, Holmgren GS, Danielsson AK, Sandgren O, Uchino M, Ando M. A new simple and rapid screening method for variant transthyretin-related amyloidosis. *Biochem Biophys Res Commun* 1996; **228**: 180–483.
- Gertz MA, Comenzo R, Falk RH, Fermand JP, Hazenberg BP, Hawkins PN, Merlini G, Moreau P, Ronco P, Santhorawala V, Sezer O, Solomon A, Grateau G. Definition of organ involvement and treatment response in immunoglobulin light chain amyloidosis (AL): a consensus opinion from the 10th International Symposium on Amyloid and Amyloidosis. *Am J Hematol* 2005; **79**: 319–328.
- Nakajima K, Okuda K, Yoshimura M, Matsuo S, Wakabayashi H, Imanishi Y, Kinuya S. Multicenter cross-calibration of I-123 metaiodobenzylguanidine heart-to-mediastinum ratios to overcome camera-collimator variations. *J Nucl Cardiol* 2014; **21**: 970–978.
- Nakajima K, Okuda K, Matsuo S, Yoshita M, Taki J, Yamada M, Kinuya S. Standardization of metaiodobenzylguanidine heart to mediastinum ratio using a calibration phantom: effects of correction on normal databases and a multicentre study. *Eur J Nucl Med Mol Imaging* 2012; **39**: 113–119.
- Hamon D, Algalarrondo V, Gandjbakhch E, Extramiana F, Marijon E, Elbaz N, Selhane D, Dubois-Rande JL, Teiger E, Plante-Bordeneuve V, Damy T, Lellouche N. Outcome and incidence of appropriate implantable cardioverter-defibrillator therapy in patients with cardiac amyloidosis. *Int J Cardiol* 2016; **222**: 562–568.
- Brignole M, Auricchio A, Baron-Esquivias G, Bordachar P, Boriani G, Breithardt OA, Cleland J, Deharo JC, Delgado V, Elliott PM, Gorenek B, Israel CW, Leclercq C, Linde C, Mont L, Padeletti L, Sutton R, Vardas PE, Guidelines ESCCfP, Zamorano JL, Achenbach S, Baumgartner H, Bax JJ, Bueno R, Dean V, Deaton C, Erol C, Fagard R, Ferrari R, Hasdai D, Hoes AW, Kirchhof P, Knuuti J, Kolh P, Lancellotti P, Linhart A, Nihoyannopoulos P, Piepoli MF, Ponikowski P, Sirnes PA, Tamargo JL, Tenders M, Torbicki A, Wijns W, Windecker S, Document R, Kirchhof P, Blomstrom-Lundqvist C, Badano LP, Aliyev F, Bansch D, Baumgartner H, Bsata W, Buser P, Charron P, Daubert JC, Dobreanu D, Faerstrand S, Hasdai D, Hoes AW, Le Heuzey JY, Mavrakis H, McDonagh T, Merino JL, Nawar MM, Nielsen JC, Pieske B, Poposka L, Ruschitzka F, Tenders M, Van Gelder IC, Wilson CM. 2013 ESC guidelines on cardiac pacing and cardiac resynchronization therapy: the Task Force on cardiac pacing and resynchronization therapy of the European Society of Cardiology (ESC). Developed in collaboration with the European Heart Rhythm Association (EHRA). *Eur Heart J* 2013; **34**: 2281–2329.
- Ruberg FL, Maurer MS, Judge DP, Zeldenrust S, Skinner M, Kim AY, Falk RH, Cheung KN, Patel AR, Pano A, Packman J, Grogan DR. Prospective evaluation of the morbidity and mortality of wild-type and V122I mutant transthyretin amyloid cardiomyopathy: the Transthyretin Amyloidosis Cardiac Study (TRACS). *Am Heart J* 2012; **164**: 222–228.e1.
- Maurer MS, Hanna M, Grogan M, Dispenzieri A, Witteles R, Drachman B, Judge DP, Lenihan DJ, Gottlieb SS, Shah SJ, Steidley DE, Ventura H, Murali S,

- Silver MA, Jacoby D, Fedson S, Hummel SL, Kristen AV, Damy T, Planté-Bordeneuve V, Coelho T, Mundayat R, Suhr OB, Waddington Cruz M, Rapezzi C. Genotype and phenotype of transthyretin cardiac amyloidosis: THAOS (Transthyretin Amyloid Outcome Survey). *J Am Coll Cardiol* 2016; **68**: 161–172.
21. Tanaka M, Hongo M, Kinoshita O, Takabayashi Y, Fujii T, Yazaki Y, Isobe M, Sekiguchi M. Iodine-123 metaiodobenzylguanidine scintigraphic assessment of myocardial sympathetic innervation in patients with familial amyloid polyneuropathy. *J Am Coll Cardiol* 1997; **29**: 168–174.
22. Nakata T, Shimamoto K, Yonekura S, Kobayashi N, Sugiyama T, Imai K, Iimura O. Cardiac sympathetic denervation in transthyretin-related familial amyloidotic polyneuropathy: detection with iodine-123-MIBG. *J Nucl Med* 1995; **36**: 1040–1042.
23. Delahaye N, Dinanian S, Slama MS, Mzabi H, Samuel D, Adams D, Merlet P, Le Guludec D. Cardiac sympathetic denervation in familial amyloid polyneuropathy assessed by iodine-123 metaiodobenzylguanidine scintigraphy and heart rate variability. *Eur J Nucl Med* 1999; **26**: 416–424.
24. Berk JL, Suhr OB, Obici L, Sekijima Y, Zeldenrust SR, Yamashita T, Heneghan MA, Gorevic PD, Litchy WJ, Wiesman JF, Nordh E, Corato M, Lozza A, Cortese A, Robinson-Papp J, Colton T, Rybin DV, Bisbee AB, Ando Y, Ikeda S, Seldin DC, Merlini G, Skinner M, Kelly JW, Dyck PJ, Diflunisal Trial Consortium. Repurposing diflunisal for familial amyloid polyneuropathy: a randomized clinical trial. *JAMA* 2013; **310**: 2658–2667.
25. Coelho T, Maia LF, Martins da Silva A, Waddington Cruz M, Planté-Bordeneuve V, Lozeron P, Suhr OB, Campistol JM, Conceição IM, Schmidt HH, Trigo P, Kelly JW, Labaudinière R, Chan J, Packman J, Wilson A, Grogan DR. Tafamidis for transthyretin familial amyloid polyneuropathy. *Neurology* 2012; **79**: 785–792.
26. Coelho T, Adams D, Silva A, Lozeron P, Hawkins PN, Mant T, Perez J, Chiesa J, Warrington S, Tranter E, Munisamy M, Falzone R, Harrop J, Cehelsky J, Bettencourt BR, Geissler M, Butler JS, Sehgal A, Meyers RE, Chen Q, Borland T, Hutabarat RM, Clausen VA, Alvarez R, Fitzgerald K, Gamba-Vitalo C, Nochur SV, Vaishnav AK, Sah DW, Gollob JA, Suhr OB. Safety and efficacy of RNAi therapy for transthyretin amyloidosis. *N Engl J Med* 2013; **369**: 819–829.
27. Maurer MS, Grogan DR, Judge DP, Mundayat R, Packman J, Lombardo I, Quyyumi AA, Aarts J, Falk RH. Tafamidis in transthyretin amyloid cardiomyopathy: effects on transthyretin stabilization and clinical outcomes. *Circ Heart Fail* 2015; **8**: 519–526.